Quantum transduction of a superconducting qubit in an electro-optomechanical and an electro-optomagnonical system

Roson Nongthombam,* Pooja Kumari Gupta,† and Amarendra K. Sarma‡
Department of Physics, Indian Institute of Technology Guwahati, Guwahati 781039, India

(Received 25 May 2023; accepted 25 September 2023; published 4 October 2023)

We study the quantum transduction of a superconducting qubit to an optical photon in electro-optomechanical and electro-optomagnonical systems. The electro-optomechanical system comprises a flux-tunable transmon qubit coupled to a suspended mechanical beam, which then couples to an optical cavity. Similarly, in an electro-optomagnonical system, a flux-tunable transmon qubit is coupled to an optical whispering gallery mode via a magnon excitation in a yttrium iron garnet ferromagnetic sphere. In both systems, the transduction process is done in sequence. In the first sequence, the qubit states are encoded in coherent excitations of phonon (magnon) modes through the phonon-qubit (magnon-qubit) interaction, which is nondemolition in the qubit part. We then measure the phonon (magnon) excitations, which reveal the qubit states, by counting the average number of photons in the optical cavities. The measurement of the phonon (magnon) excitations can be performed at regular intervals of time.

DOI: 10.1103/PhysRevA.108.043501

I. INTRODUCTION

"Quantum networks" are a rapidly developing area owing to their potential applications in scaling up quantum computers by connecting multiple quantum processors [1,2]. Recently, much research has been initiated on developing a modular quantum computer based on linking multiple superconducting chips where each chip has a few high-quality qubits. Instead of putting more qubits onto a single chip, which will result in high error rates and complex hardware, creating a network of modules containing a few high-quality qubits on a single chip is better [3–5]. This modular quantum computing approach has lower error rates and fewer hardware constraints. In order to connect the modules, optical fibers, having low propagation loss in a noisy thermal environment, are employed. The qubit operations must first be transferred to the flying optical photons in the optical fiber. The transduction of the qubit to the optical photon cannot be achieved directly due to the vast separation of the frequencies between the two (a qubit has frequency in GHz, while an optical photon has it in THz). One way to achieve transduction is by introducing a bosonic system as a mediator that couples both the qubit and the optical photon, forming a hybrid qubit-boson-optical system [6,7]. In this work, we discuss transduction in two such hybrid systems, namely, electro-optomechanical and electro-optomagnonic systems. The electro-optomechanical system consists of a superconducting microwave circuit coupled to a mechanical resonator which in turn is connected to an optical cavity. In recent years, this hybrid system has been extensively studied experimentally [8–12] and theoretically [13–20] for microwave-to-optical photon transduction. There are several ways of coupling a transmon qubit, formed by a superconducting microwave circuit, to a mechanical resonator [21–25]. Here we consider a flux-tunable transmon qubit that is coupled to a suspended mechanical beam [26]. The mechanical beam is then integrated as an end mirror of an optomechanical cavity forming the required hybrid system [17].

The hybrid electro-optomagnonic system consists of a superconducting microwave circuit coupled to a ferromagnetic magnon excitation [27–30], which is coupled to an optical photon [31–35]. This hybrid system is less explored. It is mainly due to the weak coupling between the magnon and the optical photon. However, there has been some progress recently [36]. For example, enhancement of magnon-photon coupling under the triple resonance condition of input photon, magnon, and output photon is demonstrated in [33,37]. By implementing the triple resonant condition, a microwave-to-optical conversion based on multiple magnon mode interaction with the optical photon mode is demonstrated in [38]. Another theoretical study to improve the magnon-optical coupling based on optical optical whispering gallery mode (WGM) coupled to localized vortex magnon mode in a magnetic microdisk is done in [39].

In this work, we construct the hybrid electro-optomagnonical system by merging the schemes proposed in [34] and in [37]. In the former, a flux-tunable transmon qubit is coupled to a magnon mode formed in a μm-sized yttrium iron garnet (YIG) sphere, while in the latter an optical WGM interacting with magnon mode in a YIG sphere of radius having a few hundred μm is experimentally demonstrated. One main difficulty in realizing the proposed hybrid system may occur due to the size gap in the YIG spheres. However, the possibility of reducing the sphere used in the optomagnonic case is pointed out in [37]. Assuming this to be possible, we consider a YIG sphere of a few

*n.roson@iitg.ac.in
†pooja.kumari@iitg.ac.in
‡aksarma@iitg.ac.in

μm-sized radius that couples both the superconducting qubit and the optical WGM present in the sphere.

The technique used here for measuring the qubit states from the optical photon is similar to the one employed in [10]. The idea is to first associate or encode the qubit states in the magnon (phonon) coherent excitations and then measure these excitations by counting the average number of the photon in the optical cavity. Although measuring the qubit states by detecting the optical photon count is demonstrated in [10], our scheme exhibits two distinct features. First, the interaction of the qubit and the magnon (phonon) commutes with the intrinsic Hamiltonian of the qubit. In other words, the initial state of the qubit remains the same during the interaction. Second, due to the coherent and oscillatory evolution of the magnon (phonon) and photon states during the interaction, we can perform measurements of the qubit states from the photon count at regular intervals of time.

The paper is organized as follows. We describe the two hybrid systems under study in Sec. II. The first sequence of the transduction process, i.e., encoding the qubit state in the magnon (phonon) coherent excitation, is studied in Sec. III A. The measurement of the qubit state from the optical photon count is done in Sec. III B. Finally, we conclude by summarizing our work in Sec. IV.

II. THE HYBRID SYSTEM

We first consider the hybrid electro-optomechanical system. This hybrid system comprises a flux-tunable transmon [formed by a SQUID loop (E_J, Φ_J)], coupled to a mechanical resonator [realized by suspending one arm of another SQUID loop (E_M, Φ_M)] [26] which can oscillate out of plane. The suspended mechanical membrane is then integrated as an end mirror of an optical cavity forming an optomechanical cavity [17], as shown in Fig. 1(a). The Hamiltonian of the system is described by

$$\hat{H}_{\rm eom} = \hat{H}_0 + \hat{H}_{\rm tm} + \hat{H}_{\rm om} + \hat{H}_d, \tag{1}$$

where

$$\hat{H}_0 = \hbar\Delta_c \hat{a}^\dagger \hat{a} + \hbar\omega_m \hat{b}^\dagger \hat{b} + \hbar\omega_t \hat{c}^\dagger \hat{c} - \frac{E_c}{2}\hat{c}^\dagger \hat{c}^\dagger \hat{c}\hat{c}, \tag{2a}$$

$$\hat{H}_{\rm tm} = \hbar g_{\rm tm} \hat{c}^\dagger \hat{c}(\hat{b} + \hat{b}^\dagger), \tag{2b}$$

$$\hat{H}_{\rm om} = \hbar g_{\rm om} \hat{a}^\dagger \hat{a}(\hat{b} + \hat{b}^\dagger), \tag{2c}$$

$$\hat{H}_d = \hbar E_0 (\hat{a} + \hat{a}^\dagger). \tag{2d}$$

Here $\hat{a}(\hat{a}^\dagger)$, $\hat{b}(\hat{b}^\dagger)$, and $\hat{c}(\hat{c}^\dagger)$ are the annihilation (creation) operators of the optical photon, the mechanical phonon, and the transmon, respectively. $\hat{H}_0$ is the Hamiltonian of the individual components of the hybrid system in the absence of any interactions. The transmon-mechanical resonator interaction is described by $\hat{H}_{\rm tm}$, and the optomechanical interaction by $\hat{H}_{\rm om}$. The strength of the coupling constant $g_{\rm om}$ is generally quite small ($\approx$1 Hz). So we drive the optomechanical cavity to increase the coupling strength. This drive is included in the Hamiltonian of the hybrid system as $\hat{H}_d$. The Hamiltonian $\hat{H}_{\rm om}$ is written in the optomechanical drive frame ($\Delta_c = \omega_c - \omega_d$, where ω_c is the cavity frequency and ω_d is the drive frequency.). The qubit-mechanical and optomechanical interactions arise from the displacement of the mechanical resonator. On application of an in-plane magnetic field B_z, as shown in Fig. 1(a), the displacement of the mechanical resonator picks up a flux in the Josephson energy. This motional-dependent Josephson energy leads to the transmon-mechanical resonator interaction $\hat{H}_{\rm tm}$ [26]. Note that in addition to the third-order nonlinear interaction term, $\hat{H}_{\rm tm}$, higher order nonlinear interaction terms are present as demonstrated in [26]. Here we have excluded these higher order corrections due to their negligible contribution to the system dynamics. The mechanical motion of the resonator also simultaneously alters the resonator frequency of the optomechanical cavity, which results in the optomechanical interaction $\hat{H}_{\rm om}$. We have considered a small simple harmonic motion (SHM) displacement of the resonator.

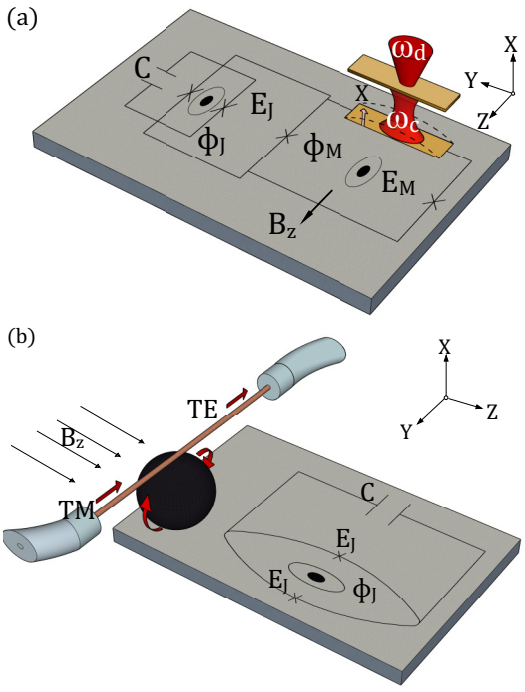

FIG. 1. (a) Schematic diagram of an electro-optomechanical system. On application of an in-plane magnetic field B_z, the transmon qubit formed by a SQUID loop (E_J, Φ_J) is coupled to a mechanical beam suspended at one arm of the loop (E_M, Φ_M) [26]. The mechanical resonator is integrated as a movable plate of an optomechanical cavity whose resonance frequency is ω_c. The optomechanical cavity is shined on by a red-detuned laser light. (b) A YIG ferromagnetic sphere that supports both the magnon excitation and optical WGM is placed near a flux-tunable transmon qubit formed by the loop (E_J, Φ_J) [34]. An optical channel is mounted on top of the YIG sphere. A TM-polarized light given at the input of the channel passes the YIG sphere in a clockwise direction, and a TE-polarized light emerges at the channel output. An in-plane magnetic field B_z, responsible for the transmon-magnon coupling, is passed through the ferromagnetic sphere.

We next consider the hybrid electro-optomagnonic system. In this system a YIG sphere having a diameter in the μm range is placed near a flux-tunable transmon formed by a symmetric SQUID loop (E_J, Φ_J) [34]. The YIG sphere is then mounted on an optical fiber placed just above the plane of the SQUID loop [37], as shown in Fig. 1(b). Just like in the

previous system, an in-plane magnetic field B_z is applied. This field magnetizes the magnetic sphere along the z direction. Because of this magnetization, a uniform magnetostatic mode or Kittel mode is excited on the YIG sphere, whose magnetic moment produces a stray field and traverse along the transmon SQUID loop. Subsequently, the stray field picks up an additional flux in the loop thereby changing the Josephson energy and frequency of the transmon and eventually leading to a transmon-magnon interaction (refer to [34] for further information on the transmon-magnon interaction). On the other hand, a TM (transverse magnetic field) polarized light is pumped at the input of the optical waveguide. When in resonance, this pumped light or signal is confined in the YIG sphere forming whispering gallery mode (WGM) in the clockwise direction. The TM input signal then interacts with the magnons in the magnetic sphere [37]. This interaction has two significant features. One is that it changes the TM-polarized input signal to a circulating TE WGM and then comes out as a TE-polarized signal at the output. The other feature is that it changes the input and output signal frequencies. The amount of change in the input and output signal frequencies is equivalent to that of the magnon frequency. The above two features are the outcomes of satisfying the triple-resonance condition (refer to [33,37] for the triple-resonance condition). The triple resonance condition is experimentally demonstrated in a 100–300 μm size ferromagnetic sphere [37]. In our case, the size of the sphere is considered to be around 3 μm. Although the size we have considered here is not yet experimentally realized for the triple resonance interaction, the possibility of sizing down the sphere is pointed out in [37]. The effective Hamiltonian of the hybrid electro-optomagnonic system is described by

$$\hat{H}'_{\rm eom} = \hat{H}'_0 + \hat{H}'_t + \hat{H}'_{\rm tm} + \hat{H}'_{\rm om} + \hat{H}'_d, \tag{3}$$

where

$$\hat{H}'_0 = \hbar\omega_v \hat{a}_v^\dagger \hat{a}_v + \hbar\omega_h \hat{a}_h^\dagger \hat{a}_h + \hbar\omega'_m \hat{m}^\dagger \hat{m}, \tag{4a}$$

$$\hat{H}'_t = \hbar\omega'_t \hat{c}^\dagger \hat{c} - \frac{E_c}{2}\hat{c}^\dagger \hat{c}^\dagger \hat{c}\hat{c}, \tag{4b}$$

$$\hat{H}'_{\rm om} = \hbar g'_{\rm om}(\hat{a}_h^\dagger \hat{a}_v \hat{m} + \hat{a}_h \hat{m}^\dagger \hat{a}_v^\dagger), \tag{4c}$$

$$\hat{H}'_{\rm tm} = \hbar g'_{\rm tm} \hat{c}^\dagger \hat{c}(\hat{m} + \hat{m}^\dagger), \tag{4d}$$

$$\hat{H}'_d = \hbar E_v(\hat{a}_v e^{-i\omega_L t} + \hat{a}_v^\dagger e^{i\omega_L t}). \tag{4e}$$

Here $\hat{a}_v(\hat{a}_v^\dagger)$, $\hat{a}_h(\hat{a}_h^\dagger)$, $\hat{m}(\hat{m}^\dagger)$, and $\hat{c}(\hat{c}^\dagger)$ are the annihilation (creation) operators of the input TM optical photon, the output TE optical photon, the magnon, and the transmon, respectively. $\hat{H}'_0$ and $\hat{H}'_t$ are the Hamiltonian of the individual components of the hybrid system in the absence of any interactions. The transmon-magnon interaction is described by $\hat{H}'_{\rm tm}$ and the optomagnonic interaction by $\hat{H}'_{\rm om}$. Here the interaction term $\hat{H}'_{\rm tm}$ is for the symmetric SQUID loop. $\hat{H}'_d$ is the optical drive of the TM mode.

III. TRANSDUCTION

Here we discuss the quantum transduction of qubit states to optical photons via mechanical phonons or YIG sphere magnons. The transduction process is realized in sequence. First, we encode the qubit states to the phonon (magnon) excitations, and next, we measure these excitations by counting the average number of photons in the optical cavity. This section is divided into two parts. The first part discusses the process of encoding the qubit states in the mechanical phonon states, and in the second part, we discuss how the phonon states, and hence the qubit states, are determined from the optical photon number.

A. Qubit-phonon (qubit-magnon) transduction

We first consider the qubit-mechanical interaction in the hybrid electro-optomechanical system and show how qubit states can be encoded to the phonon excitations. The qubit-mechanical coupling rate $g_{\rm tm}$ is much larger than the single-photon optomechanical coupling rate $g_{\rm om}$. So, if there is no optomechanical cavity drive, we can neglect the optomechanical interaction in the Hamiltonian given by Eq. (2). Now we are left with just the electromechanical part of the hybrid system:

$$\hat{H}_{em} = \hat{H}_0 + \hbar g_{\rm tm} \hat{c}^\dagger \hat{c}(\hat{b} + \hat{b}^\dagger). \tag{5}$$

Here the coupling constant $g_{\rm tm}$ is dependent on the external flux bias Φ_m as [26]

$$g_{\rm tm} = g_0 \sin(\phi_b), \tag{6}$$

where $\phi_b = \frac{\pi\Phi_b}{\Phi_0}$ and $\Phi_0 = \frac{h}{2e}$ is the flux quantum. g_0 is coupling constant. It is dependent on the transmon impedence, SQUID asymmetry, and applied magnetic field [26]. Next, we enhance the coupling rate by modulating it parametrically by applying a weak ac bias $\phi_b = \phi_{\rm ac}\cos(\omega_{\rm ac}t)$ ($\phi_{\rm ac} \ll 1$) as done in [34]:

$$g_{\rm tm} = g_0\phi_{\rm ac}\cos(\omega_{\rm ac}t). \tag{7}$$

By substituting this modulated time-dependent coupling constant in the Hamiltonian (5), and then transforming the resultant Hamiltonian in the reference frame of the ac drive ($U = e^{i\omega_{\rm ac}t\hat{b}^\dagger\hat{b}}$), we get

$$\hat{H}'_{\rm em} = \hat{H}_0 + \hbar g_0\phi_{\rm ac}\hat{c}^\dagger\hat{c}(\hat{b} + \hat{b}^\dagger) - \omega_{\rm ac}\hat{b}^\dagger\hat{b}. \tag{8}$$

Here we have ignored the fast rotating terms since $2\omega_{\rm ac} \gg g_0\phi_{\rm ac}$. To do the qubit transduction, we convert the transmon to a transmon qubit by considering only the first two energy levels. We then let the system evolve under resonant modulation ($\omega_m = \omega_{\rm ac}$). If the qubit is initially in the ground state $|g\rangle$ and the mechanical resonator is in the vacuum state $|0_b\rangle$, then after some time t, the qubit will remain in the ground state and the mechanical resonator will change to a coherent state $|\beta_b = ig_0\phi_{\rm ac}t\rangle$. Similarly, if the qubit is initially in the excited state $|e\rangle$ and the resonator in the vacuum state, then the qubit will remain in the excited state, and the mechanical resonator will evolve to another coherent state $|\beta_b = -ig_0\phi_{\rm ac}t\rangle$ after some time t:

$|g, 0_b\rangle_0 \longrightarrow |g, \beta_b = g_0\phi_{\rm ac}t\rangle_t$,
$|e, 0_b\rangle_0 \longrightarrow |e, \beta_b = -ig_0\phi_{\rm ac}t\rangle_t$.

An overall phase term induced from the intrinsic qubit Hamiltonian is not included as it does not contribute to the transduction process. We see that as the system evolves, the mechanical resonator changes from a vacuum state to a coherent state, whereas the qubit state remains as it is. It is because the interaction between the qubit and the mechanical resonator

commute with the intrinsic Hamiltonian of the qubit. In other words, the interaction is "nondemolition" in the qubit part.

We next consider transduction in the electro-optomagnonic case and analyze how qubit states can be encoded to magnon excitations. Just like in the previous case, we can neglect the optomagnonic part and consider only the electro-magnonic part since the single magnon-photon coupling $g'_{\rm om}$ is much less than the transmon-magnon coupling $g'_{\rm tm}$ for no optical drive. The electro-magnonic part is described by

$$\hat{H}'_{\rm em} = \hat{H}'_0 + \hbar g'_{\rm tm}\hat{c}^\dagger\hat{c}(\hat{m} + \hat{m}^\dagger), \tag{9}$$

where

$$g'_{\rm tm} = g'_0\frac{\sin(\phi_m)}{\sqrt{|\cos(\phi_m)|}}, \tag{10}$$

where $\phi_m = \frac{\pi\Phi_m}{\Phi_0}$ and $\Phi_0 = \frac{h}{2e}$ is the flux quantum. g_0 is the coupling constant, which depends on the radius of the sphere and the distance between the sphere and the loop [34]. Similar to the previous system, here also we enhance the coupling rate by modulating it parametrically by applying a weak ac bias $\phi_m = \phi'_{\rm ac}\cos(\omega'_{\rm ac}t)$ ($\phi'_{\rm ac} \ll 1$) as done in [34].

$$g'_{\rm tm} = g'_0\phi'_{\rm ac}\cos(\omega'_{\rm ac}t). \tag{11}$$

Substituting Eq. (11) in Eq. (9) and then transforming in drive frame ($U = e^{i\omega'_{\rm ac}t\hat{m}^\dagger\hat{m}}$) gives

$$\hat{H}'_{\rm em} = \hat{H}_0 + \hbar g'_0\phi'_{\rm ac}\hat{c}^\dagger\hat{c}(\hat{m} + \hat{m}^\dagger) - \omega'_{\rm ac}\hat{m}^\dagger\hat{m}. \tag{12}$$

The fast rotating terms are neglected for $2\omega'_{\rm ac} \gg g'_0\phi'_{\rm ac}$. We now take the first two levels of the transmon and allow the system to evolve. For resonance modulation ($\omega'_m = \omega'_{\rm ac}$), we obtain results similar to that of the electro-mechanical case:

$|g, 0_m\rangle_0 \longrightarrow |g, \beta_m = ig'_0\phi'_{\rm ac}t\rangle_t$,
$|e, 0_m\rangle_0 \longrightarrow |e, \beta_m = -ig'_0\phi'_{\rm ac}t\rangle_t$.

Here $|g, 0_m\rangle_0$ and $|e, 0_m\rangle_0$ are the initial states, and $|g, \beta_m = ig'_0\phi'_{\rm ac}t$ and $|e, \beta_m = -ig'_0\phi'_{\rm ac}t\rangle_t$ are the final states of the qubit-magnonic system after time t. An overall phase is not included.

So far, we have not included the thermal environment of the mechanical resonator, optical cavity, and transmon, which will lead to the dissipation of the system. To include the noisy environment, we allow the system to evolve under the Lindblad master equation. For the electro-mechanical system

$$\begin{aligned}\dot{\hat{\rho}}_{\rm em} = &-i[\hat{H}_{\rm em}, \hat{\rho}_{\rm em}] + \Gamma\mathcal{L}[\hat{\sigma}_z] + \Gamma\mathcal{L}[\hat{\sigma}^-] \\ &+ \gamma_b(n_{\rm th} + 1)\mathcal{L}[\hat{b}] + \gamma_b n_{\rm th}\mathcal{L}[\hat{b}^\dagger],\end{aligned} \tag{13}$$

and for the electro-magnonic system

$$\begin{aligned}\dot{\hat{\rho}}'_{\rm em} = &-i[\hat{H}'_{\rm em}, \hat{\rho}'_{\rm em}] + \Gamma\mathcal{L}[\hat{\sigma}_z] + \Gamma\mathcal{L}[\hat{\sigma}^-] \\ &+\gamma_m(n'_{\rm th} + 1)\mathcal{L}[\hat{m}] + \gamma_m n'_{\rm th}\mathcal{L}[\hat{m}^\dagger],\end{aligned} \tag{14}$$

where $\mathcal{L}[\hat{o}] = (2\hat{o}\hat{\rho}\hat{o}^\dagger - \hat{o}^\dagger\hat{o}\hat{\rho} - \hat{\rho}\hat{o}^\dagger\hat{o})/2$. Here Γ is the decoherence and dephasing rate of the transmon qubit, $\gamma_b(\gamma_m)$ is the decay rate of phonon (magnon), $n_{\rm th}(n'_{\rm th})$ is the thermal phonon (magnon) number, and $\hat{\rho}_{\rm em}(\hat{\rho}'_{\rm em})$ is the density operator of the qubit-mechanical (qubit-magnonic) system. We have neglected the thermal photons of the optical cavity due to the high frequency of the optical photon. To observe the coherent excitations of phonon and magnon in the dissipating environment, we plot the Wigner functions in Fig 2. Here we observe that the Wigner functions of the phonon and magnon at some time $\tau = (3/2\pi)$ μs and for coupling constants $g_0\phi_{\rm ac} = g'_0\phi'_{\rm ac} = 2\pi$ MHz show a coherent state profile. The amplitude of the coherent states when the qubit is in the ground state is $|\beta_b = ig_0\phi_{\rm ac}\tau\rangle = |3i\rangle$ for the phonon and $|\beta_m = g'_0\phi'_{\rm ac}\tau\rangle = |3i\rangle$ for the magnon, as shown in the figure. On the other hand, when the qubit is in the excited state, the coherent amplitudes are $|\beta_b = -ig_0\phi_{\rm ac}\tau\rangle = |3i\rangle$ and $|\beta_m = -ig'_0\phi'_{\rm ac}\tau\rangle = |3i\rangle$. These changes in the amplitude of the coherent states corresponding to the qubit ground and excited states are similar to the ones that are observed in the nondissipative case.

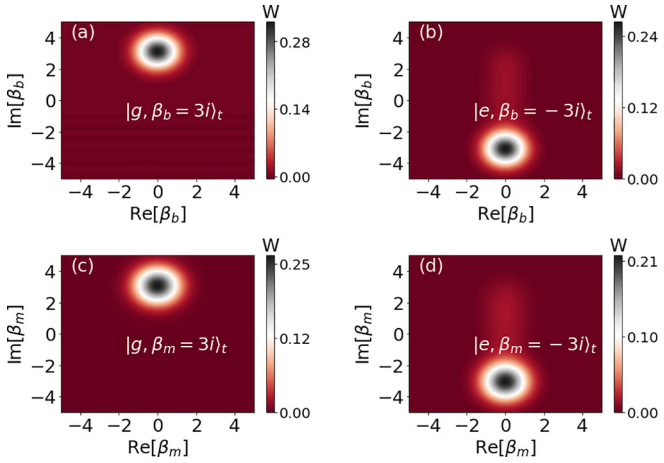

FIG. 2. Wigner function representation of the coherent states of phonon and magnon. In (a) and (c), the phonon and the magnon excites to the coherent states $|\beta_b = 3i\rangle_t$ and $|\beta_m = 3i\rangle_t$ when the qubit is in the ground state $|g\rangle$. The coherent states of the phonon $|\beta_b = -3i\rangle_t$ and the magnon $|\beta_m = -3i\rangle_t$ when the qubit is in the exited state $|e\rangle$ are shown in (b) and (d), respectively. The coherent states are taken at time $t = \tau = (3/2\pi)$ μs for coupling constants $g_0\phi_{\rm ac} = g'_0\phi'_{\rm ac} = 2\pi$ MHz. The other parameters are $\gamma_b/2\pi = 1$ Hz, $n_{\rm th} = 400$, $\gamma_m/2\pi = 0.1$ GHz, $n'_{\rm th} = 0.5$, $\Gamma/2\pi = 0.1$ GHz. The colorbar shows the Wigner function values (denoted by W) of the coherent states.

So, in both the dissipative and nondissipative qubit-mechanical and qubit-magnonic systems, we observe that the ground state of the qubit is encoded or associated with a coherent excitation of both the phonon and magnon, and the excited state of the qubit is encoded in another coherent excitation of the same magnon and phonon having amplitudes exactly opposite to that of the excitation associated with the qubit ground state.

B. Qubit-optical photon transduction

We have seen that the state of the qubit can be encoded in the coherent excitations of phonon and magnon. Here we will complete the qubit transduction sequence by transferring the phonon and magnon states to the optical photon. In the phonon case, this can be achieved through the optomechanical interaction, and in the magnon case, it can be achieved through the optomagnonic interaction satisfying the triple-resonant condition.

First, we consider the optomechanical transfer. We have previously seen from the electro-mechanical interaction that

the mechanical resonator can be coherently excited with different amplitudes depending on the initial states of the qubit. So we first excite the mechanical resonator to coherent states $|\beta_b = \pm i g_0\phi_{\rm ac} t\rangle$ and then switch off the interaction $g_0\phi_{\rm ac}$ by turning off the flux bias $\phi_{\rm ac}$. The interacting system remaining is then the optomechanical system:

$$\hat{H} = \hbar\Delta_c \hat{a}^\dagger\hat{a} + \hbar\omega_m \hat{b}^\dagger\hat{b} + \hbar g_{\rm om}\hat{a}^\dagger\hat{a}(\hat{b}^\dagger + \hat{b}) + \hbar E_0(\hat{a}^\dagger + \hat{a}). \tag{15}$$

Since $g_{\rm om} \approx 1$ Hz is very weak, we drive the cavity with an intense laser. Because of this strong drive, we can separate the amplitudes of the mechanical resonator and optical cavity into a semiclassical coherent part (β, α) and a small quantum fluctuation $(\delta\hat{a}, \delta\hat{b})$ around it, i.e., $\hat{a} \to \delta\hat{a} + \alpha$ and $\hat{b} \to \delta\hat{b} + \beta$. We substitute this separation in Eq. (15). At the steady state, the semiclassical coherent parts are given by

$$\alpha = \frac{E_0}{\kappa/2 - i\Delta_c + i(\beta + \beta^*)g_{\rm om}}, \tag{16a}$$

$$\beta = \frac{i g_{\rm om}|\alpha|^2}{\gamma_b/2 + i\omega_m}. \tag{16b}$$

In a typical experiment, the magnitude of α is of the order 10^3. By retaining only the interacting term, which is multiplied by the factor $\alpha(|\alpha| \approx 10^3)$, the Hamiltonian (15) reads

$$\hat{H}_{\rm om} = \hbar\Delta'\hat{a}^\dagger\hat{a} + \hbar\omega_m\hat{b}^\dagger\hat{b} + \hbar G_{\rm om}(\hat{a}^\dagger + \hat{a})(\hat{b}^\dagger + \hat{b}), \tag{17}$$

where $\Delta = \Delta_c - (\beta + \beta^*)g_{\rm om}$ and $G_{\rm om} = g_{\rm om}|\alpha|$ for a constant phase preference of alpha. For simplicity we have rewritten $\delta\hat{a}$ to $\hat{a}$ and $\delta\hat{b}$ to $\hat{b}$. Note that while writing Eq. (17), we have ignored all the constant terms and all the linear terms containing $\hat{a}$, $\hat{a}^\dagger$, $\hat{b}$, and $\hat{b}^\dagger$ are equated to zero [7].

The coherent state of the mechanical resonator prepared from the electro-mechanical interaction is in the mechanical frame $\omega_m = \omega_{\rm ac}$. So we transform the Hamiltonian (17) in the mechanical frame. We further transform the system in the cavity detuning frame Δ. Therefore, for a red-detuned laser drive $\Delta = \omega_m$, Eq. (17) becomes

$$\hat{H}_{\rm om} = \hbar G_{\rm om}(\hat{a}^\dagger\hat{b} + \hat{b}^\dagger\hat{a}). \tag{18}$$

Here the fast rotating terms are ignored provided $G_{\rm om} \ll 2\omega_m$. For studying the state transfer from mechanical phonon to optical photon, we write the dynamics of average number of photon and phonon in the presence of dissipation:

$$\frac{d\langle\hat{a}^\dagger\hat{a}\rangle}{dt} = -i(\langle\hat{a}^\dagger\hat{b}\rangle - \langle\hat{b}^\dagger\hat{a}\rangle)G_{\rm om} - \kappa\langle\hat{a}^\dagger\hat{a}\rangle, \tag{19a}$$

$$\frac{d\langle\hat{b}^\dagger\hat{b}\rangle}{dt} = -i(\langle\hat{b}^\dagger\hat{a}\rangle - \langle\hat{a}^\dagger\hat{b}\rangle)G_{\rm om} - \gamma_b\langle\hat{b}^\dagger\hat{b}\rangle + \gamma_b n_{\rm th}, \tag{19b}$$

$$\frac{d\langle\hat{a}^\dagger\hat{b}\rangle}{dt} = \frac{-(\kappa + \gamma_b)}{2}\langle\hat{a}^\dagger\hat{b}\rangle - iG_{\rm om}(\langle\hat{a}^\dagger\hat{a}\rangle - \langle\hat{b}^\dagger\hat{b}\rangle). \tag{19c}$$

By choosing the initial state of the mechanical resonator as the coherent state $|\beta_b(0)\rangle$ prepared from the electro-mechanical interaction, the average number of photon in the absence of dissipation is given by

$$\langle\hat{a}^\dagger\hat{a}(t)\rangle = (g_0\phi_{\rm ac}\tau)^2[1 - \sin(2G_{\rm om}t)] \tag{20}$$

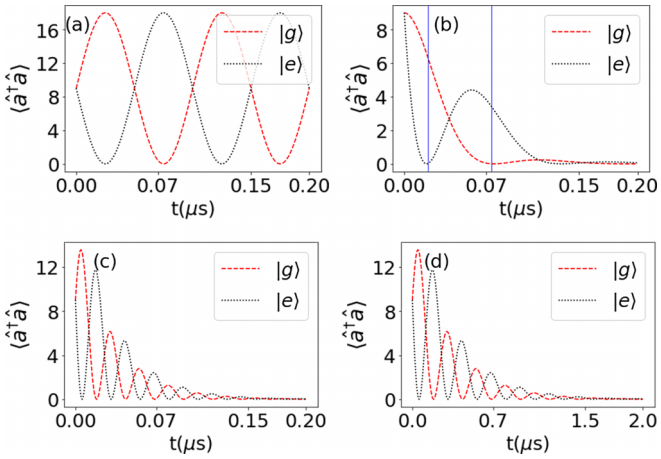

FIG. 3. Evolution of the average number of photon $\langle\hat{a}^\dagger\hat{a}\rangle$ in the optical cavity. (a) In the absence of dissipation, the oscillatory evolution of $\langle\hat{a}^\dagger\hat{a}\rangle$ keeps on going. When the qubit is in the ground state, the oscillation is represented by the dashed red line, and when the qubit is in the ground state, the oscillation is represented by the dotted black line. The evolution of average photon number in the presence of dissipation is shown in (b) for $\kappa = 2G_{\rm om}$, (c) and (d) for $2\kappa = G_{\rm om}$. In (a), (b), and (c), $\kappa/2\pi = 0.01$ GHz is used, and in (d), $\kappa/2\pi = 1$ MHz is used. The other common parameters are $\gamma = 1$ Hz and $n_{\rm th} = 400$.

when the qubit is in the ground state $(|\beta_b(0)\rangle = |+ ig_0\phi_{\rm ac}\tau\rangle)$, and

$$\langle\hat{a}^\dagger\hat{a}(t)\rangle = (g_0\phi_{\rm ac}\tau)^2[1 + \sin(2G_{\rm om}t)] \tag{21}$$

when the qubit is in the excited state $(|\beta_b(0)\rangle = |- ig_0\phi_{\rm ac}\tau\rangle)$. Here we have taken the initial state of the cavity photon to be $|\alpha(0)\rangle = |g_0\phi_{\rm ac}\tau\rangle$. The reason for choosing this particular initial state is discussed in the Appendix. The evolution of the average photon number is shown in Fig. 3(a). From the figure, we observe that if we measure the average photon number in the cavity at the interval of $t = \pi/2G_{\rm om}$ (starting from $t = \pi/4G_{\rm om}$), then we either detect or do not detect the presence of photons depending on the state of the qubit. If we detect photons in the cavity at the interval of $t = (2n+1)\pi/4G_{\rm om}$, where $n = 0, 2, 4, \ldots$, then we know that the qubit is in the ground state, and if at the same interval, we do not detect any photons, then the qubit is in the excited state. Similarly, if we detect photons in the cavity at the interval of $t = (2n+1)\pi/4G_{\rm om}$, where $n = 1, 3, 5, \ldots$, then we know that the qubit is in the excited state, and if at the same interval, we do not detect any photons, then the qubit is in the ground state. We have chosen the above particular intervals because the average photon numbers at these intervals are at the maximum separation, and the qubit states can be determined more efficiently than the other intervals.

In the presence of dissipation, the oscillatory nature of $\langle\hat{a}^\dagger\hat{a}(t)\rangle$ decays with time, and in order to know the state of the qubit by counting the photon number we require that the optomechanical coupling rate $G_{\rm om}$ should be comparable to the decay rate κ of the cavity. In Fig. 3(b) we show the decay of cavity photon number for $\kappa = 2G_{\rm om}$, a moderate coupling strength. At this coupling strength, we are able to make an efficient measurement of qubit states at just two intervals,

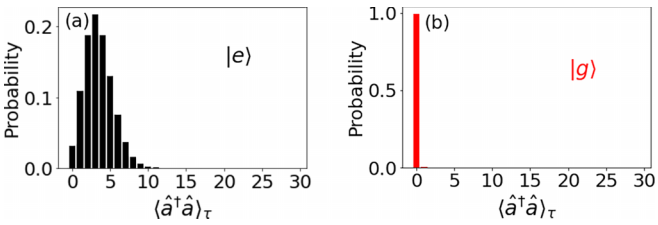

FIG. 4. Probability distribution of coherent states of the optical photon number in the presence of dissipation. (a) and (b) Distribution when the qubit is in the ground and excited state, respectively. The coherent states are measured at time $\tau = 0.075$ μs. The average photon number in (a) is 3.4 and 0 in (b).

$t = 0.02$ μs and $t = 0.075$ μs, before the number of average photon decay to zero. At a coupling strength lower than this, we will not be able to identify the qubit states from the optical photon. We also plot the case when the coupling strength is twice the decay rate in Fig. 3(c). Here more oscillations can be seen, and hence more time intervals to measure the qubit states. Furthermore, we can increase the time period for a same number of oscillations by decreasing the decay rate κ as shown in Fig. 3(d).

One could go on and find the fidelity of state transfer of coherent state from the mechanical phonon to the optical photon. However, in our case, it is not necessary since our purpose of determining the qubit state is achieved by simply counting the cavity photon number. Since we are dealing with coherent states, we can quantify how well the measured photon number indicates that the qubit is in a particular state. In Fig. 4 we plot the probability distribution of the coherent state for the $\kappa = 2G_{\rm om}$ coupling case [Fig. 3(b)] at the measurement time $\tau = 0.075$ μs. We see that even when the qubit is in the excited state, there is still some probability of not finding any photons in the cavity. The difference in the probability of not finding photons in the cavity when the qubit is in the excited state ($P_e = 0.035$) and when it is in the ground state ($P_g = 0.999$) gives the efficiency of determining the qubit state, $P = P_e - P_g = 0.964$. This efficiency decreases for less average photon number and vice versa. So we need to repeat the counting measurement several times before concluding the nature of the qubit state.

We now move on to the optomagnonic state transfer. Just like in the optomechanical case, we first excite the magnon to coherent state $|\beta_m = \pm i g'_{\rm om}\phi'_{\rm om} t\rangle$ for some time t, and then switch off the interaction $g'_{\rm om}\phi'_{\rm om}$ by turning off the flux bias $\phi'_{\rm om}$. The remaining optomagnonic system in the drive frame then reads

$$\hat{H}'_{\rm om} = \hbar\delta_v \hat{a}_v^\dagger \hat{a}_v + \hbar\delta_h \hat{a}_h^\dagger \hat{a}_h + \hbar\omega'_m \hat{m}^\dagger \hat{m} + \hbar E_v(\hat{a}_v + \hat{a}_v^\dagger) \times \hbar g'_{\rm om}(\hat{a}_h^\dagger \hat{a}_v \hat{m} + \hat{a}_h \hat{m}^\dagger \hat{a}_v^\dagger), \tag{22}$$

where $\delta_h = \omega_h - \omega_L$ and $\delta_v = \omega_v - \omega_L$. We write the dynamics of the system:

$$\frac{d\hat{m}}{dt} = -\left(\frac{\gamma_m}{2} + i\omega'_m\right)\hat{m} + ig'_{\rm om}\hat{a}_h\hat{a}_v^\dagger, \tag{23a}$$

$$\frac{d\hat{a}_v}{dt} = -\left(\frac{\kappa_v}{2} + i\delta_v\right)\hat{a}_v + ig'_{\rm om}\hat{a}_h\hat{m}^\dagger + iE_v, \tag{23b}$$

$$\frac{d\hat{a}_h}{dt} = -\left(\frac{\kappa_h}{2} + i\delta_h\right)\hat{a}_h + ig'_{\rm om}\hat{a}_v\hat{m}. \tag{23c}$$

Here γ_m, κ_v, and κ_h are the decay rates of magnon, input TM field, and output TE field, respectively. The intrinsic magnon-photon coupling rate $g'_{\rm om}$ is of the order of 10Hz, which is relatively very weak. We can enhance this coupling strength up to the order of MHz by performing an optical drive (E_v) to the ferromagnetic sphere. After the drive, we can separate the input field into semiclassical mean amplitude (α_v) and small quantum fluctuation around it ($\delta\hat{a}_v$), i.e., $\hat{a}_v \to \alpha_v + \delta\hat{a}_v$. Substituting this separation in Eq. (23) and writing the quantum and classical parts separately, we have

$$\frac{d\hat{m}}{dt} = -\left(\frac{\gamma_m}{2} + i\omega'_m\right)\hat{m} + ig'_{\rm om}(\hat{a}_h\hat{a}_v^\dagger + \hat{a}_h\alpha_v^*), \tag{24a}$$

$$\frac{d\hat{a}_v}{dt} = -\left(\frac{\kappa_v}{2} + i\delta_v\right)\hat{a}_v + ig'_{\rm om}(\hat{a}_h\hat{m}^\dagger + \alpha_h\hat{m}^\dagger), \tag{24b}$$

$$\frac{d\hat{a}_h}{dt} = -\left(\frac{\kappa_h}{2} + i\delta_h\right)\hat{a}_h + ig'_{\rm om}\hat{a}_v\hat{m}, \tag{24c}$$

and

$$\frac{d\alpha_v}{dt} = -\left(\frac{\kappa_v}{2} + i\delta_v\right)\alpha_v + iE_v. \tag{25}$$

The linear coupling terms in Eq. (24) are multiplied by a factor of α_v or α_v^* ($|\alpha_v| \approx 10^3$) compared to the nonlinear coupling terms. Therefore, we can neglect the nonlinear coupling terms and retain only the linear coupling terms. The corresponding linear Hamiltonian reads

$$\hat{H}'_{\rm om} = \hbar\delta_v\hat{a}_v^\dagger\hat{a}_v + \hbar\delta_h\hat{a}_h^\dagger\hat{a}_h + \hbar\omega'_m\hat{m}^\dagger\hat{m} + \hbar G'_{\rm om}(\hat{a}_h^\dagger\hat{m} + \hat{m}^\dagger\hat{a}_h), \tag{26}$$

where $G'_{\rm om} = g'_{\rm om}|\alpha_v|$. $|\alpha_v|$ is given by the steady value of Eq. (25).

Since the initial coherent state of the magnon prepared from the electro-magnonic interaction is in the magnon frame, we transform the Hamiltonian (26) in the magnon frame. Thus, for a resonant optical drive $\delta_v = 0$, the resultant Hamiltonian of the system in the magnon as well as the output TE field frame of reference yields

$$\hat{H}'_{\rm om} = \hbar G'_{\rm om}(\hat{a}_h^\dagger\hat{m} + \hat{m}^\dagger\hat{a}_h). \tag{27}$$

Here since the interaction satisfies the triple resonance condition, we have taken $\delta_h = \omega'_m$ or $\omega_h = \omega_v + \omega'_m$ and ignored the fast-rotating terms provided $2\omega'_m \gg G'_{\rm om}$. We see that Hamiltonian (27) and (18) are identical. Therefore, the analysis that we have done for determining the qubit states in the optomechanical system is also applicable here. The dissipative and nondissipative dynamics studied in the optomechanical system and all the plots in Figs. 3 and 4 will be similar. The optomagnonic parameters that produce similar plots in Fig. 3 are $G'_{\rm om} = 0.5\kappa_h$, $\gamma_m = 0.1$ Mhz, $\kappa_h = 0.01$ GHz, and $n'_{\rm th} = 0.5$.

IV. CONCLUSION

In conclusion, we have studied quantum transduction of a superconducting flux-tunable transmon qubit in two hybrid systems: electro-optomechanical and electro-optomagnonical

systems. The realization and advancement of quantum transduction in such hybrid systems is very crucial for the development of quantum networks, quantum internet, etc. The transduction is done in two stages. First, the qubit states are encoded in the coherent excitations of a mechanical phonon or ferromagnetic sphere magnon without disturbing the qubit state (nondemolition interaction), and in the next stage these excitations are identified by counting the average number of photons in the optomechanical or optomagnonic WGM cavity. Because of the coherent interaction between the phonon (magnon) and the optical photon, the average photon number oscillates with time. The nature of the oscillation, when the qubit is in the ground state and when it is in the excited state, is exactly opposite. As a result, multiple measurements of the photon number at a regular interval of time could be made. This enables one to have information about the state of the qubit at each interval. In the presence of dissipation, the optomechanical and optomagnonical coupling strength should be at least moderately strong in order to perform any measurements before the photon number altogether decays to zero. The required coupling strength in the optomechanical system is extensively studied. But, in the optomagnonic system, the required coupling regime to perform the transduction is not yet explored. However, the possibility of obtaining optomagnonic coupling strength up to 10 MHz is discussed in [37]. One of the ways to reach such magnitude of coupling is to reduce the size of the YIG sphere to a few μm, which is comparable to the size considered in the hybrid system proposed in this work.

ACKNOWLEDGMENTS

R.N. gratefully acknowledges support of a research fellowship from CSIR, government of India. A.K.S. acknowledges the STARS scheme, MoE, government of India (Proposal ID 2023-0161).

APPENDIX: NONDISSIPATIVE DYNAMICS

The analytical solution of Eq. (19) in the absence of dissipation is given by

$$\langle \hat{a}^\dagger \hat{a} \rangle = \tfrac{1}{2}[|\alpha_0|^2 + |\beta_0|^2 + (|\alpha_0|^2 - |\beta_0|^2)\cos(2G_{\rm om}t) - i(\alpha_0^*\beta_0 - \alpha_0\beta_0^*)\sin(2G_{\rm om}t)]. \tag{A1}$$

Here $|\alpha_0|^2 = \langle \hat{a}^\dagger \hat{a} \rangle_0$ and $|\beta_0|^2 = \langle \hat{b}^\dagger \hat{b} \rangle_0$ are the initial values of the photon and phonon (magnon). The above equation can be further simplified by simply choosing $|\alpha_0|^2 = |\beta_0|^2$:

$$\langle \hat{a}^\dagger \hat{a} \rangle = |\alpha_0|^2 - {\rm Im}(\alpha_0^*\beta_0)\sin(2G_{\rm om}t). \tag{A2}$$

The initial coherent amplitudes of the phonon (magnon) is fixed at $\beta_0 = \pm i g_0 \phi_{\rm ac} \tau$. To keep the oscillatory part in Eq. (A2), which is necessary for the transduction, we require that the initial coherent amplitude of the cavity photon α_0 should have a nonzero real part. Therefore, we choose $\alpha_0 = g_0\phi_{\rm ac}\tau$. The oscillation of Eq. (A2) then becomes

$$\langle \hat{a}^\dagger \hat{a} \rangle = (g_0\phi_{\rm ac}\tau)^2[1 - \sin(2G_{\rm om}t)] \tag{A3}$$

when the qubit is in the excited state ($\beta_0 = -i g_0\phi_{\rm ac}\tau$), and

$$\langle \hat{a}^\dagger \hat{a} \rangle = (g_0\phi_{\rm ac}\tau)^2[1 + \sin(2G_{\rm om}t)] \tag{A4}$$

when the qubit is in the ground state ($\beta_0 = i g_0\phi_{\rm ac}\tau$).

[1] C. Monroe, R. Raussendorf, A. Ruthven, K. R. Brown, P. Maunz, L. M. Duan, and J. Kim, Phys. Rev. A **89**, 022317 (2014).
[2] K. Zhang, J. Thompson, X. Zhang, Y. Shen, Y. Lu, S. Zhang, J. Ma, V. Vedral, M. Gu, and K. Kim, Nat. Commun. **10**, 4692 (2019).
[3] G. Martin, MIT Tech. Rev. (2019).
[4] M. Brooks, MIT Tech. Rev. (2023).
[5] J. Gambetta, IBM Blog (2022).
[6] N. Lauk, N. Sinclair, S. Barzanjeh, J. P. Covey, M. Saffman, M. Spiropulu, and C. Simon, Quantum Sci. Technol. **5**, 020501 (2020).
[7] W. P. Bowen and G. J. Milburn, *Quantum Optomechanics* (CRC Press, Boca Raton, FL, 2015).
[8] W. Jiang, C. J. Sarabalis, Y. D. Dahmani, R. N. Patel, F. M. Mayor, T. P. McKenna, R. Van Laer, and A. H. Safavi-Naeini, Nat. Commun. **11**, 1166 (2020).
[9] M. Forsch, R. Stockill, A. Wallucks, I. Marinković, C. Gärtner, R. A. Norte, F. van Otten, A. Fiore, K. Srinivasan, and S. Gröblacher, Nat. Phys. **16**, 69 (2020).
[10] M. Mirhosseini, A. Sipahigil, M. Kalaee, and O. Painter, Nature (London) **588**, 599 (2020).
[11] C. Wang, I. Gonin, A. Grassellino, S. Kazakov, A. Romanenko, V. P. Yakovlev, and S. Zorzetti, npj Quantum Inf. **8**, 149 (2022).
[12] R. W. Andrews, R. W. Peterson, T. P. Purdy, K. Cicak, R. W. Simmonds, C. A. Regal, and K. W. Lehnert, Nat. Phys. **10**, 321 (2014).
[13] J. Wu, C. Cui, L. Fan, and Q. Zhuang, Phys. Rev. Appl. **16**, 064044 (2021).
[14] C. Zhong, X. Han, and L. Jiang, Phys. Rev. Appl. **18**, 054061 (2022).
[15] S. Barzanjeh, D. Vitali, P. Tombesi, and G. J. Milburn, Phys. Rev. A **84**, 042342 (2011).
[16] S. Krastanov, H. Raniwala, J. Holzgrafe, K. Jacobs, M. Lončar, M. J. Reagor, and D. R. Englund, Phys. Rev. Lett. **127**, 040503 (2021).
[17] O. Černotík and K. Hammerer, Phys. Rev. A **94**, 012340 (2016).
[18] R. Nongthombam, A. Sahoo, and A. K. Sarma, Phys. Rev. A **104**, 023509 (2021).
[19] A. Clerk, K. Lehnert, P. Bertet, J. Petta, and Y. Nakamura, Nat. Phys. **16**, 257 (2020).
[20] Y.-D. Wang and A. A. Clerk, New J. Phys. **14**, 105010 (2012).

[21] J. M. Fink, M. Kalaee, A. Pitanti, R. Norte, L. Heinzle, M. Davanço, K. Srinivasan, and O. Painter, Nat. Commun. **7**, 12396 (2016).
[22] Y. Chu, P. Kharel, W. H. Renninger, L. D. Burkhart, L. Frunzio, P. T. Rakich, and R. J. Schoelkopf, Science **358**, 199 (2017).
[23] A. Bienfait, K. J. Satzinger, Y. Zhong, H.-S. Chang, M.-H. Chou, C. R. Conner, É. Dumur, J. Grebel, G. A. Peairs, R. G. Povey *et al.*, Science **364**, 368 (2019).
[24] J.-M. Pirkkalainen, S. Cho, J. Li, G. Paraoanu, P. Hakonen, and M. Sillanpää, Nature (London) **494**, 211 (2013).
[25] J. D. Teufel, T. Donner, D. Li, J. W. Harlow, M. Allman, K. Cicak, A. J. Sirois, J. D. Whittaker, K. W. Lehnert, and R. W. Simmonds, Nature (London) **475**, 359 (2011).
[26] M. Kounalakis, Y. M. Blanter, and G. A. Steele, Phys. Rev. Res. **2**, 023335 (2020).
[27] Y. Tabuchi, S. Ishino, A. Noguchi, T. Ishikawa, R. Yamazaki, K. Usami, and Y. Nakamura, Science **349**, 405 (2015).
[28] D. Lachance-Quirion, S. P. Wolski, Y. Tabuchi, S. Kono, K. Usami, and Y. Nakamura, Science **367**, 425 (2020).
[29] S. P. Wolski, D. Lachance-Quirion, Y. Tabuchi, S. Kono, A. Noguchi, K. Usami, and Y. Nakamura, Phys. Rev. Lett. **125**, 117701 (2020).
[30] H. Yuan, Y. Cao, A. Kamra, R. A. Duine, and P. Yan, Phys. Rep. **965**, 1 (2022).
[31] R. Hisatomi, A. Osada, Y. Tabuchi, T. Ishikawa, A. Noguchi, R. Yamazaki, K. Usami, and Y. Nakamura, Phys. Rev. B **93**, 174427 (2016).
[32] A. Osada, A. Gloppe, R. Hisatomi, A. Noguchi, R. Yamazaki, M. Nomura, Y. Nakamura, and K. Usami, Phys. Rev. Lett. **120**, 133602 (2018).
[33] J. A. Haigh, A. Nunnenkamp, A. J. Ramsay, and A. J. Ferguson, Phys. Rev. Lett. **117**, 133602 (2016).
[34] M. Kounalakis, G. E. W. Bauer, and Y. M. Blanter, Phys. Rev. Lett. **129**, 037205 (2022).
[35] A. Osada, R. Hisatomi, A. Noguchi, Y. Tabuchi, R. Yamazaki, K. Usami, M. Sadgrove, R. Yalla, M. Nomura, and Y. Nakamura, Phys. Rev. Lett. **116**, 223601 (2016).
[36] D. Lachance-Quirion, Y. Tabuchi, A. Gloppe, K. Usami, and Y. Nakamura, Appl. Phys. Express **12**, 070101 (2019).
[37] X. Zhang, N. Zhu, C.-L. Zou, and H. X. Tang, Phys. Rev. Lett. **117**, 123605 (2016).
[38] N. Zhu, X. Zhang, X. Han, C.-L. Zou, C. Zhong, C.-H. Wang, L. Jiang, and H. X. Tang, Optica **7**, 1291 (2020).
[39] J. Graf, H. Pfeifer, F. Marquardt, and S. Viola Kusminskiy, Phys. Rev. B **98**, 241406(R) (2018).